Low threshold voltage light-emitting diode in silicon-based standard CMOS technology

Zan Dong (董 赞)*, Wei Wang (王 伟), Beiju Huang (黄北举), Xu Zhang (张 旭), Ning Guan (关 宁), and Hongda Chen (陈弘达)

State Key Laboratory on Integrated Optoelectronics, Institute of Semiconductors, Chinese Academy of Sciences, Beijing 100083, China

**Corresponding author: dongzan@semi.ac.cn*

Received February 28, 2011; accepted March 25, 2011; posted online May 31, 2011

Low-voltage silicon (Si)-based light-emitting diode (LED) is designed based on the former research of LED in Si-based standard complementary metal oxide semiconductor (CMOS) technology. The low-voltage LED is designed under the research of cross-finger structure LEDs and sophisticated structure enhanced LEDs for high efficiency and stable light source of monolithic chip integration. The device size of low-voltage LED is 45.85×38.4 (μm), threshold voltage is 2.2 V in common condition, and temperature is 27 °C. The external quantum efficiency is about 10^{-6} at stable operating state of 5 V and 177 mA.

OCIS codes: 230.2090, 250.5300, 130.3120, 060.4510.
doi: 10.3788/COL201109.082301.

In recent years, due to the limitations of conventional electrical interconnection, optical interconnection in integrated circuits has been widely studied in different types using different methods. With the need for higher bandwidth technologies in order to keep pace with the increasing demand for speed and density, intra-chip connection with full optical way has become an important research focus of the area, because it could eliminate the obstructions to catch up with Moore's law. Optical interconnection, especially all silicon (Si)-based optical interconnection, definitely plays an important role in the next generation of communication and interconnection owing to its unmatched advantages over conventional electrical interconnection. These advantages include high bandwidth, low crosstalk, high density, mature process, low cost, etc.

Si is also an important material because of its semiconductor characteristic, plentiful resources, and widespread application in today's semiconductor industry. For optical interconnection, an electrically powered light source has the pivotal position. However, Si light source is standing out from other mature Si-based optical devices[1] because most Si optical interconnections have a problem with the Si's indirect band-gap property. Various attempts have been made in the studies of Si light source, such as porous Si[2−4], Si/Si dioxide superlattices[5], and Si nano-precipitates in Si dioxide[6] in the visible light range, and erbium doping in Si[7,8], erbium doping in Si/Ge[9], light emitting from rear locally diffused solar cell[10], iron disilicide[11], Si nanocrystals[12], and dislocation loop light-emitting diode (LED)[13] in the infrared region. Among these studies, the most dazzling achievement in the Si-based light-emitting area is the first continuous-wave Raman laser[14,15]. Although these Si light sources have achieved relatively high efficiency, their complicated process and thermal stability remain the main obstacles for realizing monolithic integration with the most widely used microelectronics technology, namely, standard Si complementary metal oxide semiconductor (CMOS) technology. To solve these problems, we start based on fully standard very large scale integration (VLSI) CMOS process to design and fabricate Si-based LEDs.

From early research, p-n junction has been proved fully compatible with standard CMOS technology. The p-n junction LED could be traced back to 1955 when Newman first reported the light-emitting phenomenon[16]. Many research have been launched from this study, and there are some studies on LED fabricated by standard CMOS technology[17−21]. However, Si is not an excellent optical material because of its well-known indirect band-gap. Moreover, bulk Si shows very inefficient band-to-band radiant electron-hole recombination, so it is not practicable for making a LED based on this material. Great efforts have thus been spent to obtain useful, that is technologically viable, and efficient material in order to achieve the most direct way of fabricating photoelectron devices. Si, however, is the best adaptable light source material in Si chips. The light intensity and spectra of Si light source are within the detecting capability of Si-based photodetectors, and such LEDs have been proved capable of picosecond switching time[22]. Si CMOS technology is the most extensive semiconductor technology for manufacturing various semiconductor chips. It has both the advantages of low cost and maturity of CMOS process. Thus, using a Si-based light source is the best way of achieving opto-electronic integrated circuits (OEICs)[23,24] in Si die. Utilizing the electroluminescence (EL) characteristic of reverse bias p-n junction, we made a kind of low threshold voltage p-n junction LED powered by a common voltage power source such as normal CMOS integrated circuits. This LED is more pragmatic than those in previous work because of its lower operating voltage and better efficiency. The emission spectrum of this device ranges from visible light range to near infrared range. This covers the detection range of the Si-based photodetector, and there is little light intensity degradation after a long time of

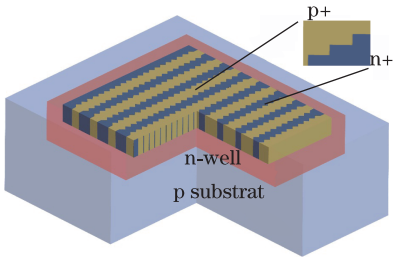

Fig. 1. Structure of the low-voltage LED.

working at room temperature. This low-voltage LED could be a fine light source for OEICs.

Our design and fabrication of LED is based on a good grasp of traditional CMOS technology. The LED takes full advantages of the mature CMOS process. The structure of the low threshold voltage LED is shown in Fig. 1.

The device is fabricated using a 0.35-μm 2P4M salicided CMOS technology without any modification. The architecture is a basic cross-finger structure with a sawtooth-shaped border of the p+ implantation and n+ implantation areas, as shown in the top right corner of Fig. 1. All the p+ implantation and n+ implantation areas are embedded in the n-well of the bulk p-substrate. The whole device is in a heavy doping area. The injection depth and concentration are optimized by the CMOS technology. All the n+ fingers and p+ fingers are connected to the cathode and anode, respectively, by contact material and metal to constitute the p-n junction of LED. A cross-finger structure could increase the border line length of the p-n junction. After many experiments of different LED structures, this structure makes the LED more efficient than other p-n junction LEDs. The total area of the low-voltage LED is 45.85×38.4 (μm). The light emits from the border, which is between the p+ implantation and n+ implantation areas. There are 10 p+ implantation fingers and the same number of n+ implantation fingers. Thus, there are 19 sawtooth-shaped bright lines which constitute the light-emitting facula of LED. Facula size is 36.35×32.2 (μm), in which the length of the cross-finger light-emitting stripe is 32.2 μm. Additionally, the space between light-emitting stripes is 1.65 μm.

Si is well known for its rich reserves, semiconductor characteristic, and indirect band-gap characteristic. It is a strait issue that let photonics emit from bulk silicon. However, researchers have worked on this issue for many years because of its perfect performance in CMOS integrate circuits. For silicon p-n junctions, when the reverse bias of the p-n junction reaches avalanching conditions, visible EL emitting phenomenon is observed. Many studies[17−21] on Si LEDs were based on this mechanism. Our previous studies[25,26] were also focused on LEDs powered by high reverse bias up to the avalanche breakdown voltage of Si p-n junction.

Luminescence occurs only when holes or electrons transit from one energy band to another. Most transitions only fall out phonons because most different quantum states of particle transition have different vectors in K-space.

Figure 2 shows that most electron-hole pairs cannot recombine directly without phonon assistance. In addition, it is shown that direct composition of electron-hole pairs

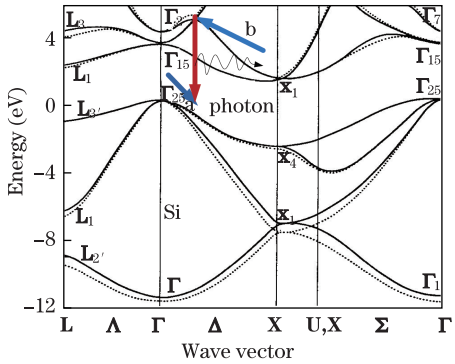

Fig. 2. Si band-gap graph in K-space **L**, **Λ**, **Γ**, **Δ**, **X**, **U**, **K**, and **Σ** are different wave vectors in simple Brillouin zone.

can only be made when there are sufficiently high energy carriers (hot carriers[27]), just like the high energy holes in Fig. 2a and the high energy electrons in Fig. 2b. Figure 2 shows the light-emitting mechanism of low-voltage LED under reverse bias. Zener breakdown caused by reverse bias supplies a large quantity of hot carriers and phonons; as shown in Figs. 2a and 2b, respectively, suitable high-energy electrons and holes recombine with the radiated photon. In previous research, avalanche breakdown comprises the majority of the reverse breakdown process. The reverse bias voltage is much higher than the avalanche breakdown voltage. For avalanche breakdown LEDs, avalanche breakdown makes a strong enough electric field so that all the electrons and holes are accelerated to hot carriers. Although the majority of hot carriers do not lead to a photon-radiative recombine, many hot carriers cause inter-band direct transition and direct radiated composition, which emit photon within the recombine action. However, many other carriers cannot get to an energy state that is high enough for direct radiated composition. Different transition processes exist as follows:

1) Intra-band direct transition. Most hot carriers do not find suitable transition partners with the same vector in K-space for photon radiation transition. As a substitute, phonon radiation is the most possible result for getting back to a low energy state.

2) Intra-band indirect transition. This transition only occurs by the intervention of phonon assistance, in which phonons are radiated mostly by intra-band direct transition.

3) Inter-band transition. Under most situations, inter-band composition is the most effective process of photon radiation. It must satisfy many conditions, such as same vector in K-space, direct transition of hot carriers, and so on.

In the present study, the breakdown of p-n junction is a way of bumping carriers to high energy bands. In contrast to the hot carrier mechanism, more photon radiation recombine occurs because of the high density of carriers in the low-voltage light-emitting process. With the increased density of electron-hole pairs, the zener breakdown process could supply enough high-energy carriers for light emission and thus decreases the threshold voltage. In standard CMOS technology, the p+ implantation and n+ implantation areas are all high-doping density areas. Thus, p+ implantation and n+ implantation

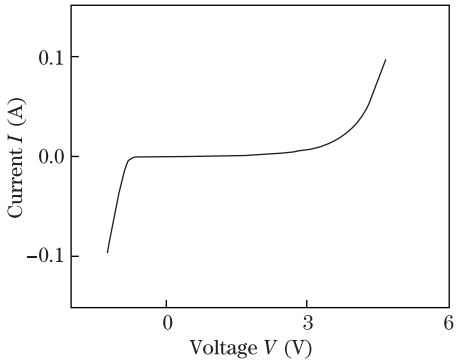

Fig. 3. Current-voltage diagram of low-voltage LED.

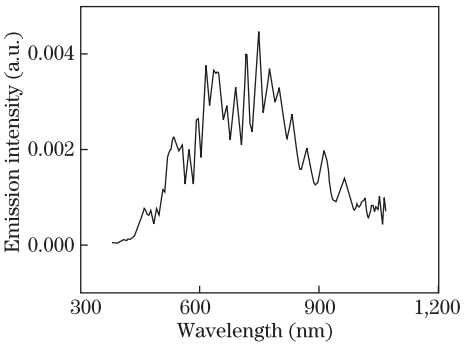

Fig. 4. Emission spectrum of the low-voltage LED.

are used for the light-emitting p-n junction. For fine p-n junction, silicide block layer must be used because quite a number of carriers release phonons to get to a low energy. Although the efficiency of electro-optical conversion is still low, there is an increase in the order of magnitude compared with the results in previous work.

The low-voltage LED emits visible light when a reverse voltage bias is supplied. The typical current-voltage ($I-V$) of the fabricated Si-LED is measured as shown in Fig. 3.

The $I-V$ characteristic in the diagram shows a Zener breakdown feature with a gradual breakdown point at about 2.2 V. Different from the avalanche breakdown, the current increasing trend after breakdown is not very sharp as shown in the diagram. It is a typical zener breakdown characteristic.

The EL spectrum of the low-voltage LED is also measured (Fig. 4). There are two distinct emission peaks at 748 and 640 nm in the measurement range from 380 to 1,068 nm. No obvious phenomenon of spectral shifting is observed with different operating voltages and currents. The main peak is at 748 nm. There are many secondary peaks caused by the Si oxide layers, which are made using the metal fabrication of different layers in the standard Si CMOS process. The spectrum is mainly filled in the visible light range, and the peaks as well as form are different from those of other work on similar semiconductor LEDs[28−30]. Furthermore, the spectrum is different from the one in our previous avalanche breakdown p-n junction LEDs. For the low-voltage LED operating at 3–5 V, zener breakdown comprises the majority of the electro-optical conversion process. In 1999, Akil *et al.* proposed a multi-mechanism model[31] to explain the avalanche emission spectra of Si junctions. However, the photon generation mechanism of this low-voltage LED is still not conclusive. Both the Si/Si dioxide in nanometer size and the defect in Si would be the hosts for catalyzing radiative recombine. Perhaps different hosts are the causes, which then lead to photons emitting at different wavelengths. In the current experiment, the EL spectrum remains stable for a long time, and the photon energy at 748 and 640 nm are results of the recombination by hot carriers. Further research needs to be conducted to obtain a fundamental understanding of the mechanism behind the emission of the devices. This is the best way to optimize the performance of the devices.

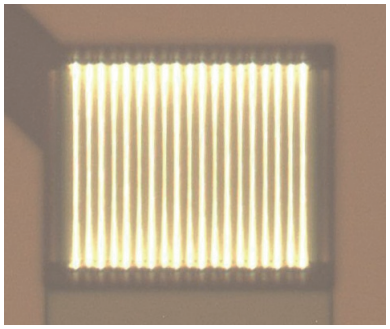

Fig. 5. Microscope graph of low-voltage LED.

By accumulating EL spectral data, the output power of the low-voltage LED is obtained. The microscope graph in Fig. 5 shows that the output power is about 19.3 nW, as detected by the spectral measurement equipment at a reverse bias of 4.9 V. The whole optical output is actually greater than this. A great amount of output power dissipated during the measurement because of the dispersion by Si oxide layers and optical lens.

The graph of the low-voltage LED in light-emitting state in the experiment is taken via the Olympus microscope. In Fig. 5, the while light can be clearly seen by naked eyes. The exposure time of Fig. 5 is 0.5 s; thus, the facula is a little overflowing at the strong area, similar to the top and bottom of the whole facula. The sawtooth shape could not be seen for the same reason. In Fig. 5, the LED's operating voltage is about 4.9 V with a breakdown reverse current of 167 mA at room temperature. When the operating current turns down, the output power of the LED varies linearly with the input current. Moreover, the working current of LED could be altered in a small range when the temperature changes if it is powered by a permanent voltage source. The facula also can be seen by the naked eyes. External quantum efficiency of the low-voltage LED is about 10^{-6}, which has an order of magnitude increase using the new design. For the stability test, the LEDs are kept working for about 3 h in the heat sinker, and show that they work well in the experiment. Both the stability and the intensity of the low-voltage LED make the device feasible for OEIC applications, as well as suitable as the light source for optical communication in monolithic chips.

In conclusion, a novel low-voltage LED made by all-Si standard CMOS technology is demonstrated. To the best of our knowledge the structure of Zener breakdown p-n junction is the first successful application on Si LED in standard CMOS technology without any modification. It is based on many designs and experiments from previous work. The LEDs, which have good stability and high integrability, can be used as the light sources of new

OEICs and other new applications in monolithic chips. We are thus looking forward to a brand-new era that will be brought about by Si photonics.

This work was supported by the National Natural Science Foundation of China (Nos. 61036002, 60536030, 60776024, 60877035, 61076023, and 90820002) and the National "863" Program of China (Nos. 2007AA04Z329, 2007AA04Z254, 2011CB933203, and 2011CB933102).

References

1. A. E. Willner, L. Zhang, Y. Yue, and X. Wu, Chin. Opt. Lett. **08,** 909 (2010).
2. L. T. Canham, Appl. Phys. Lett. **57,** 1046 (1990).
3. Y. Kanemitsu, K. Suzuki, S. Kyushin, and H. Matsumoto, Phys. Rev. B **51,** 13103 (1995).
4. H. Khatun, S. S. Mou, A. A. Mortuza, and A. B. M. Ismail, Chin. Opt. Lett. **8,** 306 (2010).
5. Z. H. Lu, D. J. Lockwood, and J. M. Baribeau, Solid Store Electron. **40,** 197 (1996).
6. T. Komoda, J. Kelly, E. Cristiano, A. Nejirn, P. L. F. Hemment, K. P. Homewood, R. Gwilliam, J. E. Mynard, and R. J. Scal, Nucl. Inst. Meth. B **96,** 387 (1995).
7. G. Franzò, F. Priolo, S. Coffa, A. Polman, and A. Carnera, Appl. Phys. Lett. **64,** 2235 (1994).
8. T. D. Chen, A. Agarwal, L. M. Giovane, J. S. Foresi, L. Liao, D. R. Lim, M. T. Morse, E. J. Ouellette III, S. H. Ahn, X. Duan, J. Michel, and L. C. Kimerling, Proc. SPIE **3279,** 136 (1998).
9. H. Presting, H. Kibbel, M. Jaros, R. M. Turton, U. Menczigar, G. Abstreiter, and H. G. Grimmeiss, Semicond. Sci. Tech. **7,** 148 (1992).
10. M. A. Green, J. Zhao, A. Wang, P. J. Reece, and M. Gal, Nature **412,** 805 (2001).
11. D. Leong, M. Harry, K. J. Resson, and K. P. Homewood, Nature **387,** 686 (1997).
12. M. Xie, Z. Yuan, B. Qian, and L. Pavesi, Chin. Opt. Lett. **7,** 319 (2009).
13. W. L. Ng, M. A. Lourenco, R. M. Gwilliam, S. Ledain, G. Shao, and K. P. Homewood, Nature **410,** 192 (2001).
14. H. Rong, A. Liu, R. Jones, O. Cohen, D. Hak, R. Nicolaescu, A. Fang, and M. Paniccia, Nature **433,** 292 (2005).
15. L. Pavesi, Materials Today **8,** 18 (2005).
16. R. Newman, Phys. Rev. **100,** 700 (1955).
17. L. W. Snyman, A. Biber, H. Aharoni, M. Plessis, B. D. Patterson, and P. Seitz, in *Proceedings of Workshop on High Performance Electron Devices for Microwave and Optoelectronic Applications* 340 (1997).
18. L. W. Snyman, H. Aharoni, and M. Plessis, IEEE Photon. Technol. Lett. **17,** 2041 (2005).
19. H. Aaroni and M. Plessis, IEEE J. Quantum Electron. **40,** 557 (2004).
20. L. W. Snyman, M. Plessis, and H. Aharoni, Jpn. J. Appl. Phys. **46,** 2474 (2007).
21. L. W. Snyman, K. A. Ogudo, M. Plessis, and G. Udahemuka, Proc. SPIE **7208,** 72080C (2009).
22. J. C. Tsang, J. A. Kash, and D. P. Vallett, IBM J. Res. Develop. **44,** 583 (2000).
23. L. W. Snyman, H. Aharoni, A. Biber, A. Bogalecki, L. Canning, M. Plessis, and P. Maree, Proc. SPIE **3953,** 20 (2000).
24. S. Sayil, in *Proceedings of IEEE Region 5 Technical Conference* 42 (2007).
25. H. Chen, H. Liu, J. Liu, M. Gu, and B. Huang, Chin. Phys. Lett. **24,** 265 (2007).
26. B. Huang, X. Zhang, Z. Dong, W. Wang, and H. Chen, in *Proceedings of 9th International Conference on Solid-State and Integrated-Circuit Technology* 20 (2008).
27. J. Bude, N. Sano, and A. Yoshii, Phys. Rev. B **45,** 5848 (1992).
28. J. Kramer, P. Seltz, E. F. Stelgmeler, H. Auderset, and B. Delley, Sensor. Actuator. Phys. **37-38,** 521 (1993).
29. C. W. Liu, S. T. Chang, W. T. Liu, M. Chen, and C. Lin, Appl. Phys. Lett. **77,** 4347 (2000).
30. M. Plessis, H. Aharoni, and L. W. Snyman, IEEE J. Sel. Top. Quantum Electron. **8,** 1412 (2002).
31. N. Akil, S. E. Kerns, D. V. Kerns, A. Hoffmann, and J. P. Charles, IEEE Trans. Electron Dev. **46,** 1022 (1999).